BACKGROUND REJECTION AND DATA ANALYSIS FOR THE PAMELA EXPERIMENT

Aldo Morselli [a] and Piergiorgio Picozza [a]

[a] *INFN, Sezione di Roma II, via della Ricerca Scientifica, Roma, Italy and Dipartimento di Fisica, Università di Roma "Tor Vergata", via della Ricerca Scientifica, Roma, Italy*

Abstract

PAMELA is a satellite-borne experiment which will measure the antiparticle component of cosmic rays over an extended energy range and with unprecedented accuracy. The apparatus consists of a permanent magnetic spectrometer equipped with a double-sided silicon microstrip tracking system and surrounded by a scintillator anticoincidence system. A silicon-tungsten imaging calorimeter, complemented by a scintillator shower tail catcher, and a transition radiation detector perform the particle identification task. Fast scintillators are used for Time-Of-Flight measurements and to provide the primary trigger. A neutron detector is finally provided to extend the range of particle measurements to the TeV region. PAMELA will fly on-board of the Resurs-DK1 satellite, which will be put into a semi-polar orbit in 2005 by a Soyuz rocket. We give a brief review of the scientific issues of the mission, the developement of the background rejection and data analysis programs and report about the status of the experiment few months before the launch.

1 The beginning of Cosmic Ray Physics, the balloons

The direct measurement of Cosmic Ray started for INFN around the 1989 with the beginning of the activity of the WiZard Collaboration, described in [1]. In table 1 there are the balloon flights launched after that date both by the WiZard Collaboration (on the left) and of the other collaboration (BESS, HEAT, IMAX), using novel techniques developed for accelerator physics.

Beginning from 1995, the WiZard Collaboration and the AMS Collaboration begun to launch also space detectors. The list is given in table 2 together with other connected space experiments.

The summary of all the data collected up to now for the antiproton and positron absolute flux are shown in [2].

Table 1: Second generation balloon flights (on the left the flights of the WiZard collaboration)

WiZard collaboration	Others Collaborations
MASS (89, 91)	BESS (93, 95, 97, 98, 2000)
TrampSI (93)	Heat (94, 95, 2000)
CAPRICE (94, 97, 98)	IMAX (96)
	BESS Long duration flight (2004)

Table 2: Space experiments for the measurement of cosmic rays

*	**Cosmic rays**		
√	SilEye-1	MIR	1995-1997
√	SilEye-2	MIR	1997-2001
√	AMS-01	Shuttle	1998
√	NINA-1	Resurs	1998
√	NINA-2	MITA	2000
√	Alteino (SilEye-3)	ISS	2002 (April 25)
▷	PAMELA	ResursDK1	2005
▷	AMS-02	ISS	2008
*	**Low energy γ-ray**		
√	HETE-2	Pegasus	2002 (Jan 14)
√	INTEGRAL	Proton	2002 (Oct 17)
▷	SWIFT	Delta II	2004
▷	AGILE	MITA	2005
▷	GLAST	Delta II	2007
*	**UHE cosmic rays**		
▷	EUSO	ISS	2008

1.1 The PAMELA experiment

PAMELA (Payload for Antimatter Matter Exploration and Light-nuclei Astrophysics) will be mounted in a dedicated Pressurized Container (PC) attached to Resurs-DK1 to be launched in 2005 for a mission at least three years long. Dur-

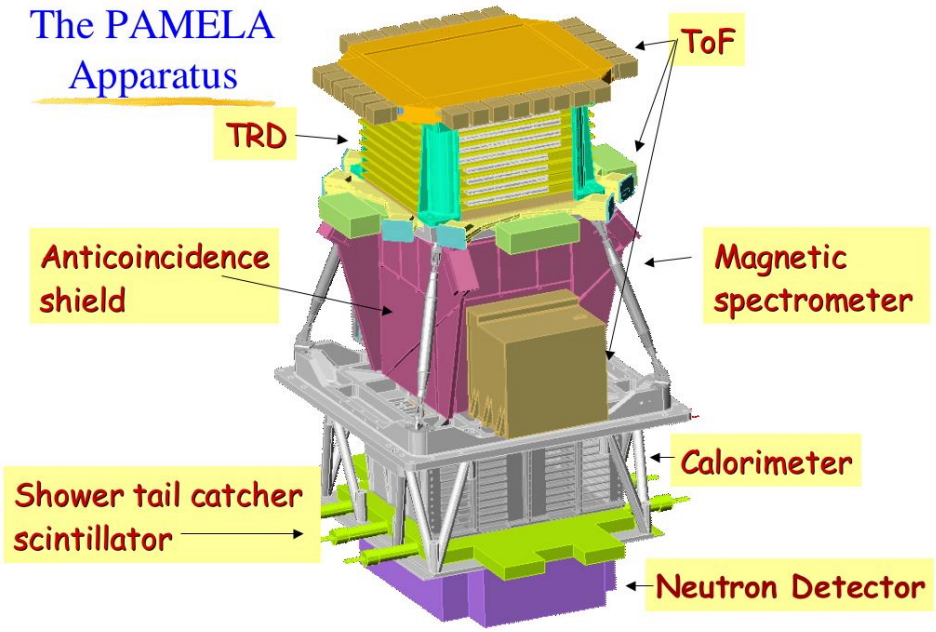

Figure 1: PAMELA apparatus.

ing launch and orbital manoeuvres the PC is secured against the satellite's body. During data-taking it will be swung up to give PAMELA a clear view into space.

This satellite will execute a semipolar, elliptical orbit with an inclination of 70.4° and an altitude varying between 350 and 600 km.

The list of the people and the Institution involved in the collaboration together with the on-line status of the project is available at *http://wizard.roma2.infn.it/*.

The PAMELA Scientific Primary goals are the search for heavy nuclei and non baryonic particles outside the Standard Model, for the understanding of the formation and evolution of our Galaxy and the Universe and for the exploring of the cycles of matter and energy in the Universe. Additional objectives of PAMELA are the study of galactic cosmic rays in the heliosphere, Solar flares, distribution and acceleration of solar cosmic rays (SCR's) in the internal heliosphere, magnetosphere and magnetic field of the Earth, stationary and disturbed fluxes of high energy particles in the Earth's magnetosphere and anomalous component of cosmic rays.

The PAMELA observations will extend the results of balloon-borne experiments over an unexplored range of energies with unprecedented statistics and will complement information gathered from Great Space Observatories.

More precisely, during its three years of planned operation, PAMELA will measure with very high statistics:

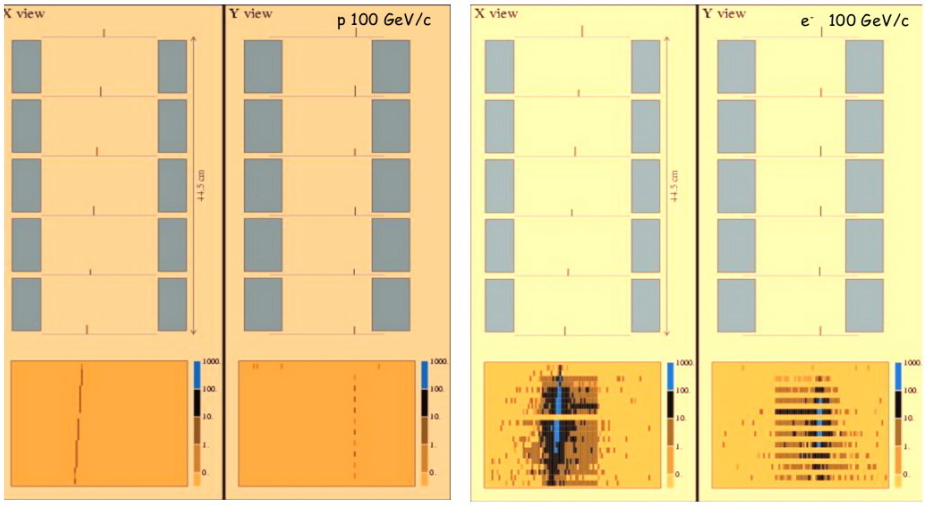

Figure 2: A non-interacting proton and an electron track recorded at the SPS 2003 beam test

- Positron flux from 50 MeV to 270 GeV (present limits 0.7 - 30 GeV)
- Antiproton flux from 80 MeV to 190 GeV (present limits 0.4 - 50 GeV)
- Limit on antinuclei $\sim 10^{-8}(\overline{He}/He)$ (present limit about 10^{-6})
- Electron flux from 50 MeV to 3TeV
- Proton flux from 80 MeV to 700 GeV
- Light nuclei flux (up to oxygen) from 100 MeV/n to 200 GeV/n
- Electron and proton components up to 10 TeV
- Continuous monitoring of the cosmic rays solar modulation

In [2] there are reported the PAMELA expectations for the antiproton and positron fluxes for standard model of production and propagation of cosmic rays.

An overview of the instrument is given in figure 1. PAMELA is built around a 0.4 T permanent magnet spectrometer (tracker) equipped with double-sided silicon detectors which will be used to measure the sign, absolute value of charge and momentum of particles. The tracker is surrounded by a scintillator veto shield (anticounters, AC) which is used to reject particles which do not pass cleanly through the acceptance of the tracker. The AC system is composed of a top detector, CAT, and four side detectors, CAS. Each detector is made from a sheet of 8mm thick plastic scintillator read out by photomultiplier tubes. The CAS detectors surround the spectrometer (tracker and magnet) and help to reject out-of-acceptance triggers. Above the tracker is a transition radiation detector made of proportional straw tubes and carbon fibre radiators. This allows electron-hadron separation through threshold velocity measurements. Mounted below the tracker is an imag-

ing silicon-tungsten calorimeter that measures the energy of incident electrons and allows topological discrimination between electromagnetic and hadronic showers (or noninteracting particles). The sampling calorimeter is made from silicon sensor planes interleaved with tungsten absorbers. The traverse resolution is given by the segmentation of the silicon detectors. The segmentation is made in 32 strips with a width of 2.4 mm. Each tungsten plane is sandwiched between two layers of silicon detectors. Either view (X or Y) is composed of a square matrix of $3 \cdot 3$ detectors and each strip is connected to the those belonging to the two detectors of the same row (or column). The data from the calorimeter front end boards are processed by four DSPs (Digital Signal Processors). One DSP takes care of data from either an even or odd numbered X or Y plane. In both the X and Y direction there are 22 planes. Each DSP is receiving signals from 11 planes (here called a sector).

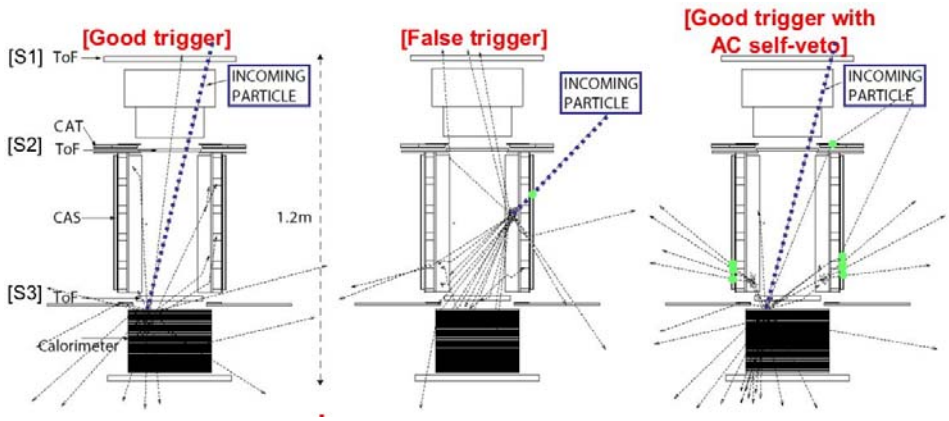

Figure 3: Event types: (left, a) a 'good' trigger, (middle, b) a 'false' trigger, (right, c) a backscattering event

A scintillator telescope system provides the primary experimental trigger and Time-Of-Flight particle identification. An additional scintillator (Bottom Scintillator, S4) is mounted beneath the calorimeter to trigger the acquisition of the neutron detector that, right at the bottom of the PAMELA detector, provides additional information to separate hadronic from electromagnetic showers up to 10 TeV. PAMELA has dimensions of approximately $75 \cdot 75 \cdot 123$ cm^3, an overall mass of 450 kg (plus about 20 kg of Gas Supply system refurbishing the TRD detector) and a power consumption of 355 W. The total geometric factor is 20.5 cm^2 sr. Tables 1 and 2 report PAMELA mass and power budget respectively. Detailed descriptions of the characteristics and functionalities of the single PAMELA subdetectors can be found in [3]. Following the standard procedure for space missions, the instrument PAMELA has been produced in three different models: Mass-Dimensional & Thermal Model (MDTM), intended for space qualification of

mechanical structure and thermal system;

Technological Model (TM), intended for check out of electrical interfaces to Resurs and basic control and data procedures; Flight Model (FM), which will undergo a minimal number of tests before being sent to space. From July 2000 until September 2003 PAMELA Flight Model was extensively exposed to beam tests at CERN PS and SPS to study its physics performance. A preliminary integrated flight model set-up consisting of the tracker and anticounting system and calorimeter was exposed to protons (200 GeV 300 GeV) and electrons (40 GeV 300 GeV) at the CERN SPS in June 2002. The TRD as stand-alone detector was also tested. Last test with an almost complete Flight Model set-up has been carried out in September 2003 again at SPS. Figure 2 show a non-interacting proton and an electron track recorded during this test beam session.

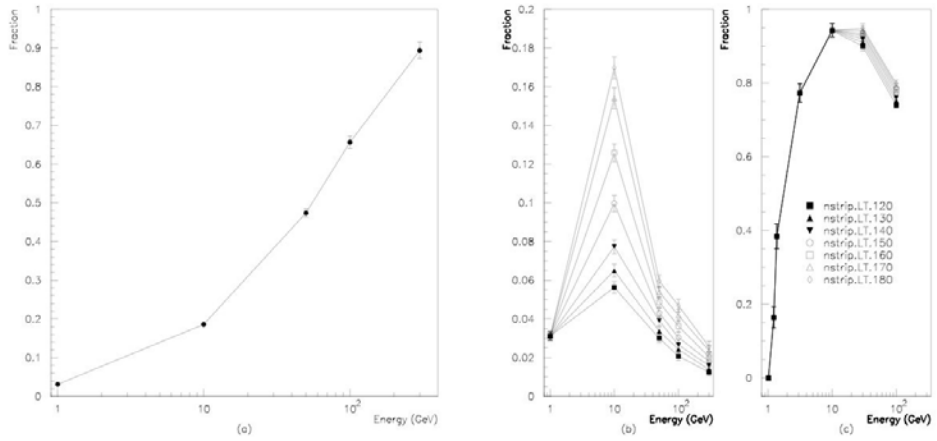

Figure 4: a) Backscattering ratio with only AC rejection (electrons), b) Backscattering ratio with combined AC and calorimeter rejection (electrons), c) Rejection ratio with combined AC and calorimeter rejection (protons)

A first level trigger can include both 'good' triggers, i.e. particles entering and traversing the tracker acceptance and reaching the calorimeter without interacting, and 'false' triggers, i.e. particles hitting the experiment from outside the acceptance or interacting with the inside of the tracker cavity. In figures 3a and 3b these two types of triggers are illustrated. To examine the performance of the AC system, a simulation study has been performed [4]. The simulations included protons of various energies generated at locations situated above, on the side of, and below the experiment. The dominant component of the 'false' triggers are produced by particles hitting the experiment from above, but a non-negligible component comes from particles hitting the experiment from the sides and from below. By using the AC system in a second level trigger one can reduce this background significantly with the condition that a level one trigger should not be

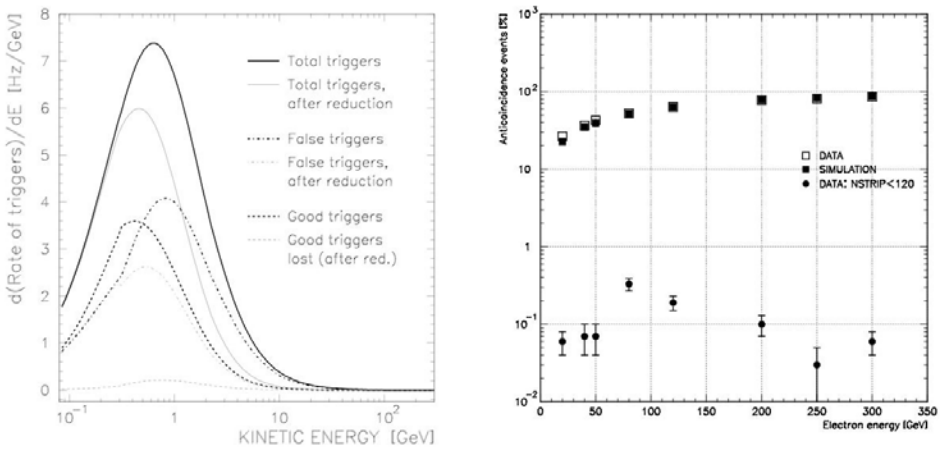

Figure 5: (left) trigger rates, (right) results from the testbeam study

accompanied by a signal in any of the AC detectors.

An event where a particle passes cleanly through the spectrometer can still give rise to an AC signal due to backscattered particles produced in the calorimeter (see figure 3c). Using the AC system to reject 'false' triggers in this simple way will therefore result in loss of 'good' events. To estimate the effect of backscattering, electrons were simulated entering the apparatus from above in the PAMELA acceptance. As shown in figure 4a the fraction of rejected 'good' triggers increases significantly with the energy of the incident particles as expected. Considering that high energy electrons are much less abundant than low energy ones it's necessary to avoid using selections that have high inefficiencys. The energy deposition in the the calorimeter was used to provide a variable sensitive to the development of the shower. The calorimeter variable used was the total number of strips that were hit for each sector (11 planes). A revised second level trigger condition was then formed, i.e.: signal in AC and no activity in any of the 4 calorimeter sectors above a predefined cut-off. A range of cut-offs were investigated from 120-180 (out of 1056) strips. In figure 4b the fraction of rejected 'good' triggers is plotted for the 8 different cuts-offs in the strip variable. As seen in this figure the fraction of lost 'good' events is greatly reduced (especially at higher energies). The effect of the these cuts on the rejection of 'false' proton triggers is shown in figure 4c.

When combined with the proton spectrum for the polar region of the orbit where the proton flux has it's maximum, the resulting trigger rate becomes as shown in figure 5(left). The total integrated trigger rate after reduction is 11.6 Hz for a cut-off of 120 strips. It can also be seen that the 'false' trigger rate can be reduced significantly (integration gives a total reduction by 70 %) without losing any significant part of the 'good' events. A test beam study was performed at CERN in the H4 beam line. An electron beam of various energies was aimed at

the center of the PAMELA acceptance. In figure 5 (right) the full circles show the measured ratio where an AC rejection combined with a calorimeter cut-off of 120 strips has been imposed. The full squares shows the same but without the calorimeter condition. They can be compared with the backscattering estimated from a simulation of the test beam AC (open squares) and a good agreement can be noticed.

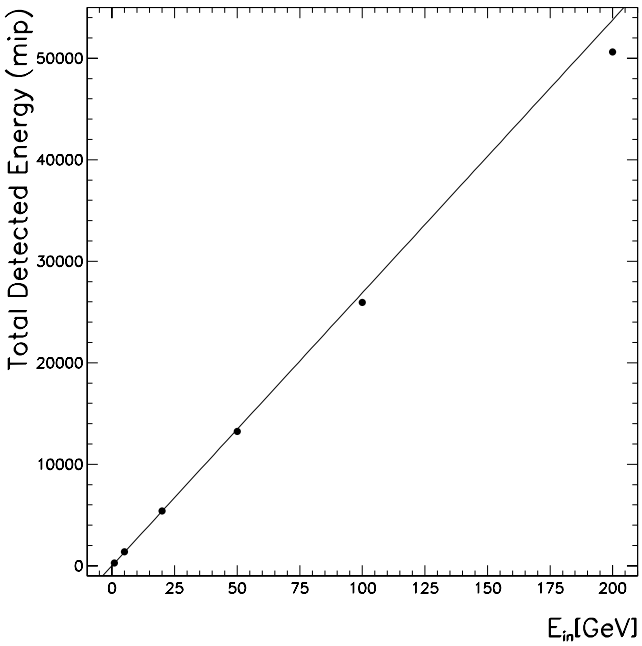

Figure 6: Reconstructed energy as a function of input energy for simulated electrons in the PAMELA configuration. The solid line is a linear fit to the first four points.

1.2 The Calorimeter

Similar silicon-tungsten calorimeters, differing only in layout and number of radiation lengths, were developed and extensively studied through simulations, beam tests [5, 6] and balloon flights [7, 8, 9]. The simulated data were compared with experimental data finding excellent agreement [5, 6, 9]. From these simulations, a Monte Carlo program based on the CERN GEANT/FLUKA-3.21 code [10] was developed to study the capability of the PAMELA calorimeter. In particular, it was studied the performance of the calorimeter concerning the primary scientific goals of the PAMELA experiment, that is energy reconstruction for electrons and identification of positrons and antiprotons in a vast background of protons and

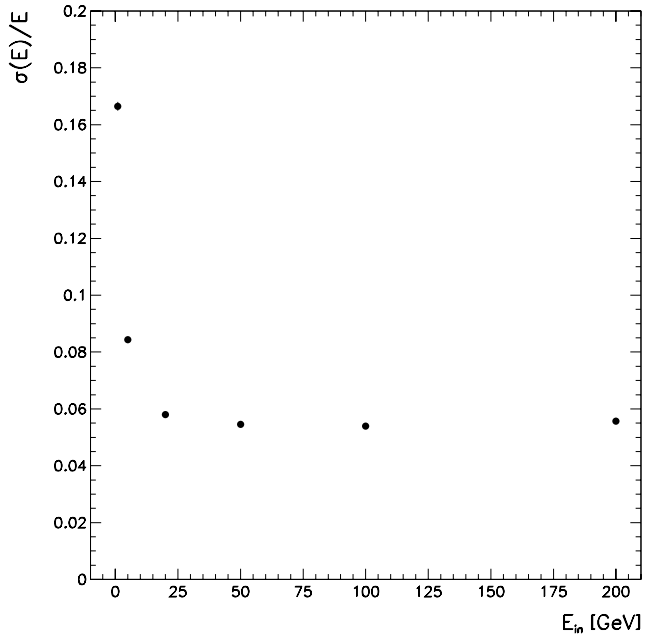

Figure 7: Energy resolution as a function of input energy for simulated electrons in the PAMELA configuration.

electrons, respectively. Figure 6 shows the simulation of the total detected energy (expressed in mip units) in the calorimeter for electrons at several energies. The response of the calorimeter, in this energy range, shows a quasi-linear behaviour with deviations accounting for the partial containment at the highest energies. The solid line is a linear fit to the simulated data points below 100 GeV. Figure 7 shows the energy resolution for electrons. The resolution reaches a constant value above 20 GeV of about 5%. In a cosmic-ray experiment like PAMELA, the proton background accounts for about 10^3 times the positron component at 1 GeV, increasing with energy to more than 10^4 above 10 GeV. Electrons are about 10^2 more abundant than antiprotons at 1 GeV, decreasing with energy but still being about 30 times more at 10 GeV. For this reason powerful particle identifiers are needed. The PAMELA calorimeter is well suited to identify these particles in the cosmic radiation (see figure 8). The longitudinal and transverse segmentation of the calorimeter combined with the measurement of the energy lost by the particle in each silicon strip results in a high identification power for electromagnetic showers. Thus, the calorimeter, in the electron and positron analysis, is used to identify electromagnetic showers, while in the antiproton analysis the calorimeter is used to reject these events.

Selection criteria were developed based on the following information of the

electromagnetic showers [6]:

1. the starting point of the shower;
2. the energy-momentum match;
3. the longitudinal profile;
4. the transverse profile;
5. the topological development of the shower.

The efficiency and contamination of the selections were studied simulating a large number of electrons (electrons and positrons were assumed to be equivalent at the energy of interest here), antiprotons and protons.

Figure 9 shows a quantity related to the topological development of the shower in the calorimeter for simulated 100 GeV/c (a) electrons and (b) protons . This quantity is the product of the sum of the number of hits inside a cylinder, of radius about 2 Molière units (8.5 calorimeter strips) with its axis along the particle direction, and the corresponding calorimeter plane number. The direction of the particle in the calorimeter was assumed known since in the PAMELA experiment it will be obtained from an extrapolation of the fitted track in the tracking system. Table 3 shows the resulting values for various momenta spanning the range of interest for PAMELA.

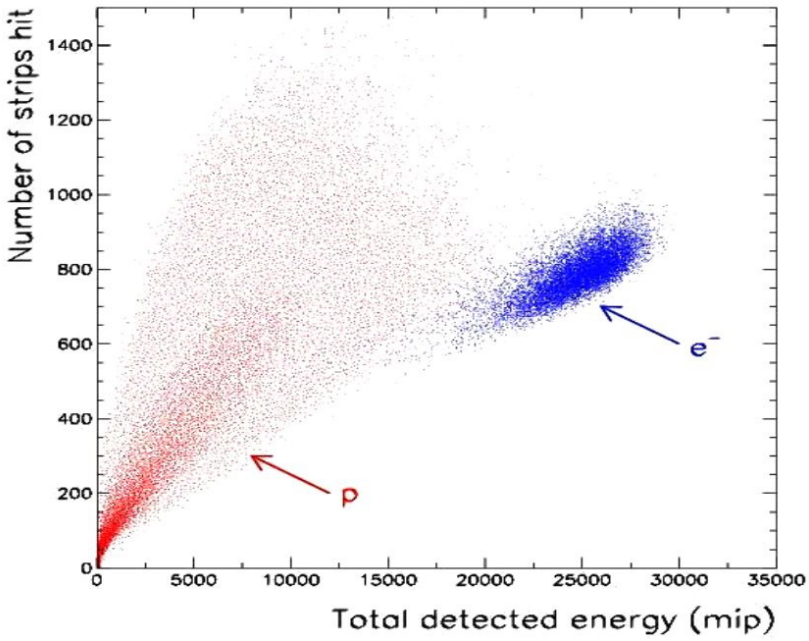

Figure 8: Electron-Proton separation from the calorimeter in the SPS Test Beam Data with 200 GeV/c protons and electrons

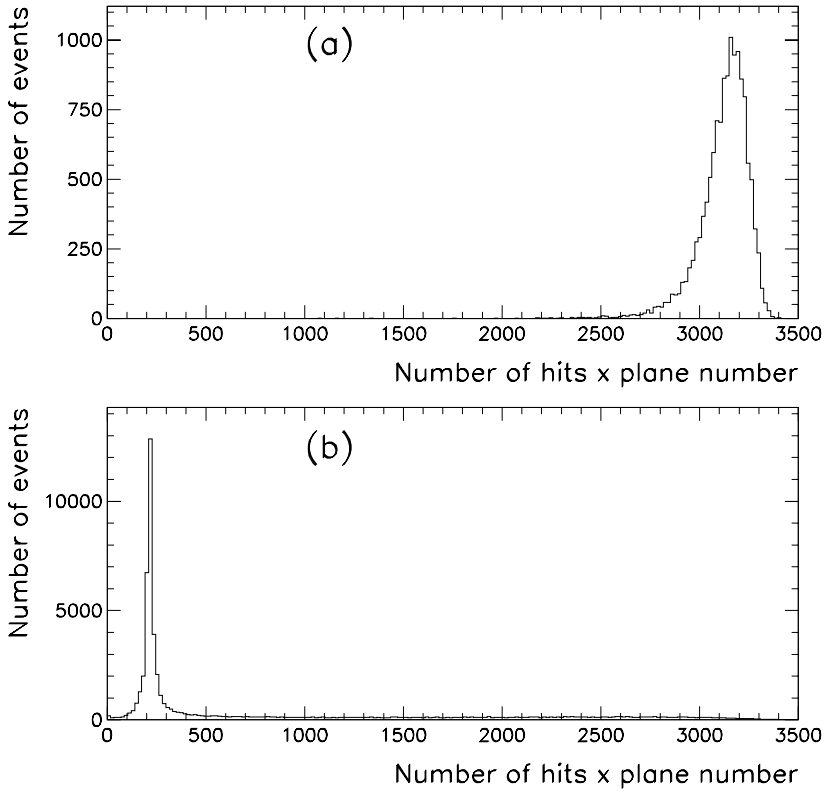

Figure 9: The topological development of the shower. The figure shows the sum of the number of hits inside 2 Molière units around the track multiplied by the corresponding calorimeter plane number for simulated 100 GeV/c (a) electrons and (b) protons.

2 Conclusion

The assembly of the instrument PAMELA is very close to its conclusion. The Mass-Dimensional & Thermal Model passed all tests for space qualification. The Technological Model assembly took more than one year and it is now concluded; the model is going to be integrated with the satellite for electrodiagnostic tests in Samara. The Flight Model system integration is under way in Rome. SPS beam tests of an almost complete setup for final calibration and tracker alignment were done in September 2003. The schedule for the next few months is very tight. After the final integration of the Flight Model, it is planned to expose PAMELA FM to a vibration test at minimal loads at IABG - Munich - for a final check of the structure. Afterwards PAMELA will fly to Samara where the final integration

Table 3: Simulated performances: efficiencies in antiproton and electron detection versus electron and proton contamination, respectively.

Momentum (GeV/c)	$\overline{\mathrm{p}}$ efficiency	e^- contamination
1	0.9192 ± 0.0009	$(2.5 \pm 0.2) \times 10^{-3}$
5	0.9588 ± 0.0005	$(4^{+5}_{-2}) \times 10^{-5}$
20	0.9767 ± 0.0004	$< 6.2 \times 10^{-5}$
100	0.963 ± 0.001	$< 1.4 \times 10^{-4}$
200	0.954 ± 0.002	$< 1.5 \times 10^{-4}$

into the satellite, together with the ancillary detectors that will be put onboard - experiments ARINA and EOS - will start. The tests in Samara will last up to 3 months, and then Resurs will reach the Baikonur launch site. The final tests in-situ will take between 8 and 12 weeks, ensuring the spacecraft launch before Summer 2005.

References

[1] P.Picozza, A.Morselli, 2003. J. Phys. G: Nucl. Part. Phys., 29, 903-911

[2] Andrea Lionetto, Aldo Morselli and Vladimir Zdravković, these proceedings

[3] O. Adriani et al., NIM A 511, 72, 2003. M. Boezio et al., NIM A 487, 407, 2002. D. Campana et al., Proc. 28th ICRC, 2141, 2003. M. Pearce et al., Proc. 28th ICRC, 2125, 2003. F. Cafagna et al., Proc. 28th ICRC, 2121, 2003.

[4] J. Lundquist, et al. , Proc. 28th ICRC, 2133, 2003.

[5] M. Bocciolini et al., Nucl. Instr. and Meth. **A333** (1993) 560.

[6] M. Boezio, Ph.D. thesis Royal Institute of Technology, Stockholm, (1998) http://msia02.msi.se/group_docs/astro/research/references.html

[7] R. Golden et al., Astrophys. J. **457** (1996) L103

[8] M. Boezio et al., Astrophys. J. **487** (1997) 415.

[9] M. Boezio et al., Astrophys. J. **532** (2000) 653.

[10] R. Brun et al, Detector Description and Simulation Tool, CERN program library